Designing an Aerial Robot for Hover-and-Stare Surveillance

Paul Y. Oh*, Michael Joyce and Justin Gallagher
Drexel University, Philadelphia PA
Email: [paul.yu.oh, michael.joshua.joyce, justin.gallagher]@drexel.edu

Summary

When disasters and crises arise visual information needs to be rapidly gathered and assessed in order to assist rescue workers and emergency personnel. Often such situations are life-threatening and people cannot safely obtain such information. Disasters in urban areas are particularly taxing. Structural collapse, damaged staircases and the loss communication infrastructures aggravate rescue efforts. Robots, equipped with camera, can be employed to visually capture situational awareness. As such, the focus of our work is designing a backpackable aerial robot that can hover-and-stare. Such a robot would ascend, peer through windows, and transmits video to an operator. This paper presents a backpackable tandem-rotor prototype that can carry a wireless camera.

Keywords: aerial robots, search-and-rescue, sensor suites, eld robotics

Figure 1: Backpackabe aerial robot prototype with on-board camera performs hover-and-stare mission outside a window

1 Introduction

Predator and Global Hawk are unmanned aerial vehicles (UAVs) that support divisions (over 2000 personnel) with high-altitude image data. By contrast, micro-air-vehicles (MAVs) denote aircraft that support a squad (up to nine personnel) at close quarters. Called a Class 1 UAV, MAVs are envisioned as rapidly deployable, backpackable, autonomous aerial robots equipped with a camera system to *hover-and-stare*. The MAV would peer through windows, over roofs or above tree canopies to support missions like search-and-rescue [1] and target acquisition. Towards this, ducted or shrouded rotary-wing candidates have been proposed, which unlike helicopters, can sustain light bumps without damaging itself or obstacles like walls and trees. It should be noted that xed-wing miniature aerial vehicles exist [2] [4] but they typically fly around 20 MPH in open skies and thus not suited for hover-and-stare.

The authors' particular research interests lie in characterizing and analytically designing sensor suites for autonomous MAVs. While some non-commercial MAV prototypes exist, few are ready to be equipped with collision avoidance sensors and flight tested in near-Earth environments. Consequently, the authors breadboarded a vehicle roughly matching the flight envelope and footprint of a Class 1 UAV to serve as a research platform. Figure 1 depicts the resulting prototype which ts in a backpack (diameter less than 20-inches), carries a 1-pound payload and transmits wireless video. One overarching design constraint was to use widely available and affordable components so that other research groups could duplicate or evolve the vehicle.

*The U.S. Army Medical Research Acquisition Activity, 820 Chandler Street, Fort Detrick, MD 21702-5014 is the awarding and administering acquisition office. This investigation was funded under a U.S. Army Medical Research Acquisition Activity; Cooperative Agreement W81XWH 04-1-0419. The content of the information herein does not necessarily reflect the position or the policy of the U.S. Government or the U.S. Army and no official endorsement should be inferred.

Component	Mass [kg]
2 Motors	0.170
Batteries	0.035
Avionics	0.029
Nacelle frame	0.100
Camera	0.015
2 RC servos	0.014
Miscellaneous	0.087
Total	**0.450**

Table 1: Weight budget for vehicle components

Breadboarding such a vehicle proved challenging because the UAV and aerial robot literature seldom provide design and fabrication details. There is little airfoil data at low Reynolds numbers [8] and the characteristics of rotary-wings, such as small-scale engines or ducted fans [7], are rarely available for MAV footprints. To help ll this gap in the knowledge base, this paper illustrates the design details of a backpackable, light-weight airframe that can robotically ascend and perform hover-and-stare tasks and structured as follows. Section 2 describes the design thresholds, constraints and footprint justifying a tandem rotor con guration; Section 3 details the construction of a test rig to collect dynamic thrust data; Section 4 highlights the fabrication of the vehicle's carbon- ber body; Section 5 presents initial flight control and stability tests; Flight tests and conclusions are given in Section 6.

2 Tandem Rotor Design

The Defense Advanced Research Projects Agency (DARPA) has been a long time advocate of MAVs. Their MAV Industry Briefs provide design thresholds and objectives that capture desired attributes. Examples for a Class 1 aircraft include tting in a backpack, weighing one pound (450-grams) or less, airlifting a half-pound or more, and sustaining light bumps into obstacles like walls. With this as a guideline, design trades were performed resulting in a shrouded tandem-wing con guration (see Figure 2). A preliminary design review for a vehicle weighing less than 1-pound (450-gram) yielded a weight budget as shown in Table 1.

Rotorcraft, like conventional helicopters, spin an airfoil to achieve lift. The angular momentum that is generated results in a counter-rotation. Often a tail rotor is used to oppose such rotation. Other methods include using two rotors that rotate in opposite direc-

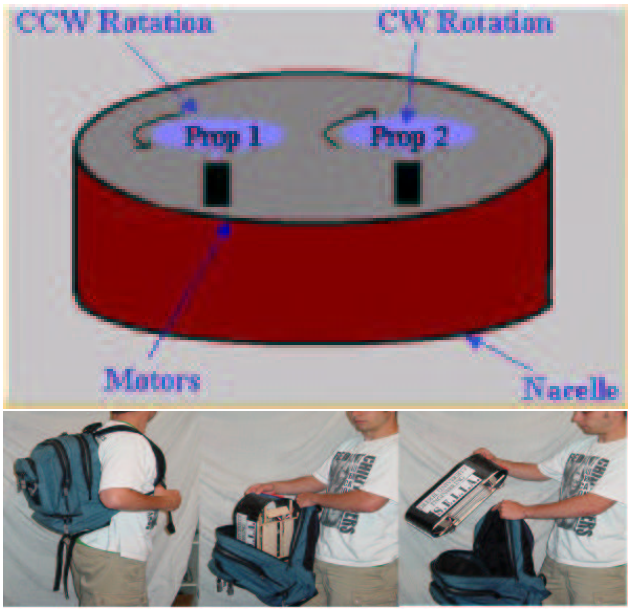

Figure 2: Counter-rotating rotors conserve angular momentum (top). By shrouding the rotors in a nacelle, the vehicle can sustain slight collisions. While using two rotors does increase vehicle size, design trades in body material and propulsion can still result in a backpackable unit that measures 17-inches long, 8-inches wide and 4-inches tall (bottom).

tions. This tandem rotor con guration is often used in heavy-lift aircraft like the Chinook helicopter where rotors are mounted at the ends of the fuselage. Alternatively, the two rotors can be mounted co-axially. While such a setup yields a smaller footprint, the resulting gearing mechanisms are often complex and require a more sophisticated flight controller.

While many factors must be considered, payload weight is an overarching one. Off-the-shelf 7 4 (7-inch length, 4-inch pitch) rotor-wing airfoils and size 480 motors are common. This translates into a pitch, $p = 4.0$ inches or $0.102\ m$ and a rotor radius, $r = 3.5$ inches or $0.089\ m$. Size 480 motor specs list an unloaded rotational velocity of $\omega = 250$ rev/s. The lift that can be generated by an airfoil attached to a DC motor is given by

$$T = \frac{1}{2}\rho V^2 A \tag{1}$$

where ρ is air density ($1.225\ kg/m^3$), V is the airfoil velocity and A is the area spanned by the rotor. Consequently

$$V = \omega p = 250\ \frac{rev}{s} \quad 0.102\ m = 25.4\ \frac{m}{s} \tag{2}$$

$$A = \pi r^2 = \pi \left(0.089\ m\right)^2 = 0.0248\ m^2 \qquad (3)$$

which yield, using (1), $T = 9.81\ N$ or the ability to theoretically airlift a total mass m_T of 1000 grams. Due to losses, an engineering rule of thumb suggests the true mass is one-third the theoretical. The net effect is that two size 480 motors in a tandem con- guration should be able to airlift $m_T = 666$ grams in practice. If the vehicle mass, $m_v = 450$ grams, the available thrust can airlift a payload mass of $m_p = m_T \quad m_v = 216$ grams (0.48 pound).

3 Dynamic Thrust Data

The preliminary design and calculations in Section 2 underscore the physics relating vehicle weight and thrust. The equations provide a rst approximation for sizing motor and propellers. Typically one over-engineers components to ensure adequate thrust. Oftentimes this results in heavier motors and larger propellers, which in turn, increases vehicle size and weight. In small backpackable aerial robots like ours, such over-engineering can lead into a vicious design cycle. To avoid this, accurate motor-propeller data is needed to narrow margins of error.

Unless thrust measurements are made under real or simulated flight conditions, they may not be realistic indications of actual performance. To be meaningful, thrust measurements needs to be dynamic, with the propeller moving through airflow as in actual flight. As such, a test rig (see Figure 3) was constructed to collect dynamic thrust data.

The test rig's free body diagram is given in Figure 4. The motor and propeller combination is attached to one end of the arm. The arm is then pivoted at a distance D from its center of mass. The arm angle, , as measured by the protractor depends on the generated thrust T. Let M be the distance between the propeller and pivot point while W is the weight of the entire test bed and motor-propeller combination.

At equilibrium, the torques generated by thrust and weight are balanced such that $DW \cos \quad = MT$. Consequently, the dynamic thrust is given by

$$T = \frac{DW \cos}{M} \qquad (4)$$

The net effect is that such a test rig allows one to rapidly collect dynamic thrust data and compare different motor-propeller combinations. Figure 5 graphically depicts the thrust for different combinations.

Figure 3: Lever arm angle as measured by the protractor (close up in upper right inset) is proportional to the rotational speed of the motor-propeller (close up in lower left inset). At equilibrium the dynamic thrust balances the torque due to gravity.

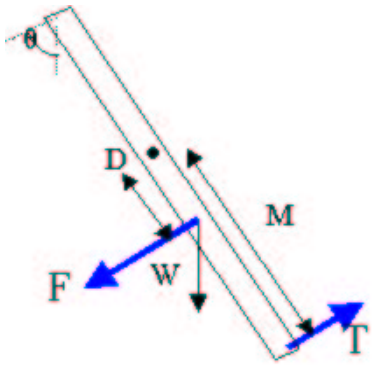

Figure 4: Free body diagram for the dynamic thrust test rig.

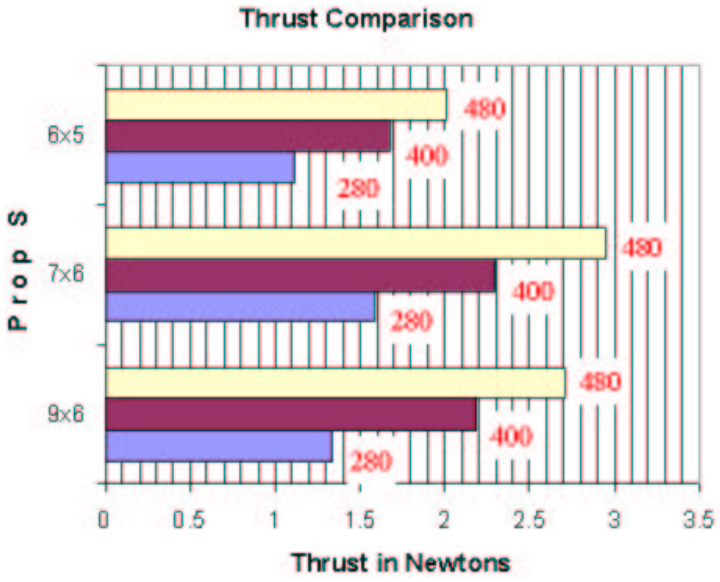

Figure 5: Thrust with different motor-propeller combinations

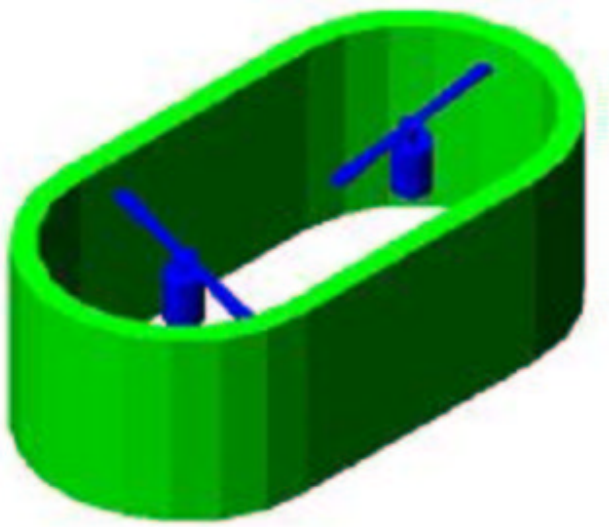

Figure 6: Given two 7 4 airfoils, the nacelle should measure 17 7 6 inches long, wide and high respectively, to suitable encase the airfoils, avionics and actuators.

From the data, a size 480 motor and 7 4 propeller will generate su cient lift for the envisioned 1-pound aerial robot.

4 Airframe Design

A nacelle is a shroud which surrounds a rotor. It acts as a protective skirt and enables the vehicle to survive light bumps into obstacles. Referring to Table 1, weight constraints dictate the nacelle be light (100 grams). An elliptical nacelle measuring 17-inches and 8-inches on major and minor axes respectively and a 6-inch height can adequately encase the two 7 4 airfoils, avionics and actuators (see Figure 6). A foam nacelle was rst considered because of the material is rigid, easy to machine, moldable, durable and semi-elastic for withstanding bumps. A mold was created and the mass of the resulting foam nacelle was 178 grams. As this exceeded the allotted weight budget a carbon ber nacelle was fabricated. Although this was a more involved process, the resulting nacelle was durable, rigid, then and an acceptable mass of 74 grams.

As discussed in Section 2, counter-rotating tandem rotors will conserve angular momentum. However, any differences between the two motors will yield unwanted vehicle yawing. Control surfaces, called baffles can compensate for such differences (see Figure 7 top).

Changes in baffle angle enable thrust to be vectored and prevent yawing. The baffles also allow the vehicle to remain hovering despite sudden gusts. The baffles and motor-propeller combination were mounted on the test rig and dynamic thrust data was collected. Figure 7 (bottom) shows that theoretical calculations (box data points) yield conservative values of thrust. Wind tunnel and test rig tests (diamond and triangle data points respectively) yield actual dynamic thrust values.

5 Control Issues

Rotorcraft control is often a challenging problem because the longitudinal and lateral flight dynamics are tightly coupled. While a tandem rotor con guration does not completely eliminate this coupling, control is greatly simpli ed. The vehicle was mounted on the test rig and a voltage step input was applied. The test arm was retro tted with an optical encoder and angle data was acquired. The open loop response is shown in Figure 8 (left), suggesting the vehicle has second order dynamics. The voltage input to angle output transfer function was identi ed as

$$G_m(s) = \frac{40.2945}{s^2 + 0.3127s + 40.2945} \qquad (5)$$

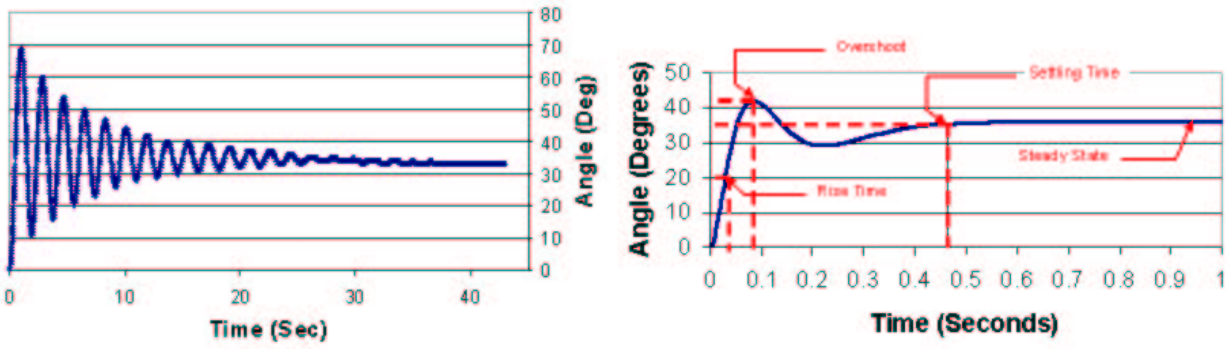

Figure 8: Open loop response of the test arm angle to step input voltage (left) reveals second order dynamics of the vehicle. Pole-placement compensator was designed and simulated closed-loop response (right) reveals reduced oscillation and quicker settling time.

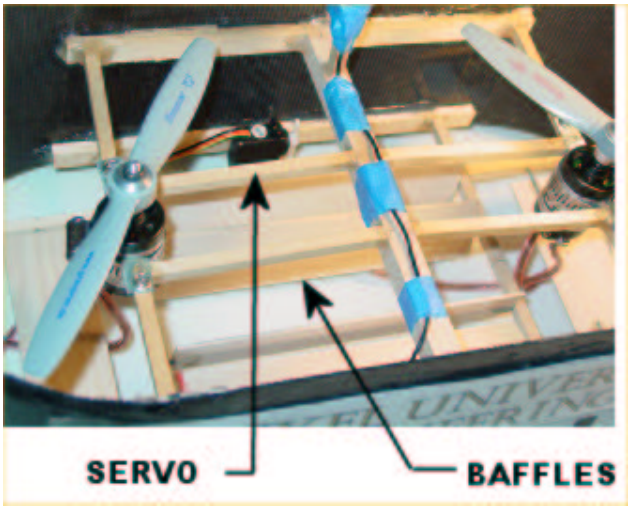

Figure 7: Thrust-vectoring is achieved by servoing the baffle angle (top). Theoretical and experimental results of dynamic thrust versus baffle angle (below).

where the natural frequency ω_n is 0.0132 rad/sec and the damping ratio ζ is 11.8446. A pole-placement compensator was designed to minimize the rise and settling times to 0.05 and 0.45 seconds respectively.

$$C(s) = \frac{0.2166s^2 + 2.298s + 17.68}{0.01167s^2 + s} \qquad (6)$$

The closed-loop response simulation is given in Figure 8 (right).

6 Conclusions

Figure 9 depicts three camera shots of the vehicle while flight testing. Power to the vehicle is delivered by two 7.4 Volt 340 mAh Lithium poly batteries but flight time is limited to about 90 seconds. Higher capacity batteries are currently reaching the market so extended flight times can be achieved. For flight testing, the vehicle is tethered to a 5 Volt 36 Amp power supply. Figure 9 (left) shows the vehicle powered hang test looking into a window and the view of the vehicle's on-board wireless camera (right).

This paper illustrated the design details of a backpackable, light-weight airframe for perform hover-and-stare tasks. A tandem rotor con guration was used to facilitate control and airlift a vehicle and payload weighing 1 and 0.5 pounds respectively. First order approximations of the lift were derived and corroborated by dynamic thrust data. A test rig was custom built to mimic air flow as in actual flight. Baffles for thrust-vectoring were designed and experimentally validated. A pole-placement controller was designed to illustrate that the vehicle's second order dynamics

Figure 9: Hang test and inside view

can be easily compensated.

Our particular interests are in designing sensor suites for such vehicles. The prototype presented in this paper can serve as a test bed to test and validate sensors. Our future goals include using miniature optic flow sensors to enable autonomous collision avoidance [10] [5] [9]

References

[1] Blitch, J., "World Trade Center Search-and-Rescue Robots", Plenary Session *IEEE Int Conf Robotics and Automation*, Washington D.C., May 2002.

[2] Ettinger, S.M., Nechyba, M.C., Ifju, P.G., Waszak, M., "Vision-Guided Flight Stability and Control for Micro Air Vehicles", *IEEE/RSJ Int Conf on Robots and Systems*, Lausanne, Switzerland, pp. 2134-2140, October 2002.

[3] Fearing, R., et al, "Wing Transmission for a Micromechanical Flying Insect", *IEEE Int Conf Robotics and Automation*, San Francisco pp. 1509-1516, April 2000.

[4] Grasmeyer, J.M., Keennon, M.T., "Development of the Black Widow Micro Air Vehicle", *39th AIAA Aerospace Sciences Meeting and Exhibit*, Reno, NV, Jan. 2001.

[5] Green, W.E., Oh, P.Y., Barrows, G., Sevcik, K., "Autonomous Landing for Indoor Flying Robots Using Optic Flow", *ASME Int. Mech. Eng. Congress and Expo.*, v2, pp. 1341-1346, Wash., D.C., Nov. 2003.

[6] Hazawa, K.; Shin, J.; et al "Autonomous flight control of hobby-class small unmanned helicopter: trajectory following control by using preview control considering heading direction", Proc. IEEE/RSJ Int. Conf. Robots and Systems (IROS), V1, pp. 754-760, Oct. 2004.

[7] Choi, H., Sturdza, P., Murray, R.M., "Design and Construction of a Small Ducted Fan Engine for Nonlinear Control Experiments", *Proc. American Control Conference*, Baltimore MD, pp. 2618-2622, June 1994.

[8] Mueller, T.J., "Aerodynamic Measurements at Low Reynolds Numbers for Fixed Wing Micro-Air Vehicles", presented at the *Development and Operation of UAVs for Military and Civil Applications*, course held at the Von Karman Institute for Fluid Dynamics, Belgium, Sept 13-17, 1999.

[9] Netter, T., Francheschini, N., "A Robotic Aircraft that Follows Terrain Using a Neuromorphic Eye", *IEEE/RSJ Int Conf on Intelligent Robots and Systems*, V1, pp. 129-134, Lausanne, Switz., Sept. 2002.

[10] Oh, P.Y., Green, W.E., "Closed Quarter Aerial Robot Prototype to Fly In and Around Buildings", *Int. Conference on Computer, Communication and Control Technologies*, Vol. 5, pp. 302-307, Orlando, FL, July 2003.